Available online at www.sciencedirect.com

ScienceDirect

Journal of Solid State Chemistry 180 (2007) 1875–1881

JOURNAL OF SOLID STATE CHEMISTRY

www.elsevier.com/locate/jssc

Two new hydrogen bond-supported supramolecular compounds assembly from polyoxovanadate and organoamines

Wei-Jie Duan[a], Xiao-Bing Cui[a], Yan Xu[b], Ji-Qing Xu[a,*], Hai-Hui Yu[a], Zhi-Hui Yi[a], Ji-Wen Cui[a], Tie-Gang Wang[a]

[a] *College of Chemistry and State Key Laboratory of Inorganic Synthesis and Preparative Chemistry, Department of Chemistry, Jilin University, Changchun 130023, China*

[b] *Institute of Chemistry for Functionalized Materials, College of Chemistry and Chemical Engineering, Liaoning Normal University, Dalian 116029, China*

Received 13 January 2007; received in revised form 15 March 2007; accepted 24 April 2007
Available online 5 May 2007

Abstract

Two novel organic–inorganic hybrid compounds based on organoamines and polyoxovanadates formulated as $(H_2dien)_4[H_{10}V_{18}O_{42}(PO_4)](PO_4)\cdot 2H_2O$ (**1**) (dien = diethylenetriamine) and $(Him)_8[HV_{18}O_{42}(PO_4)]$ (**2**) (im = imidazole) have been prepared under hydrothermal conditions by using different starting materials, and characterized by elemental analyses, IR, ESR, XPS, TGA and single-crystal X-ray diffraction analyses. Crystal data for compound **1**: $C_{16}H_{74}N_{12}O_{52}V_{18}P_2$, Monoclinic, space group $C2/c$, $a = 23.9593(4)$ Å, $b = 13.0098(2)$ Å, $c = 20.1703(4)$ Å, $\beta = 105.566(3)^\circ$, $V = 6056.6(19)$ Å^3, $Z = 4$; for compound **2**, $C_{24}H_{41}N_{16}O_{46}V_{18}P$, Tetragonal, space group $I4/mmm$, $a = 13.5154(8)$ Å, $b = 13.5154(8)$ Å, $c = 19.1136$ Å, $\beta = 90^\circ$, $V = 3491.4(3)$ Å^3, $Z = 2$. Compound **1** consists of protonated diens together with polyoxovanadates $[H_{10}V_{18}O_{42}(PO_4)]^{5-}$. Compound **2** is composed of protonated ims and polyoxovanadates $[HV_{18}O_{42}(PO_4)]^{8-}$. There are hydrogen-bonding interactions between polyoxovanadates and different organoamines in **1** and **2**. Polyoxovanadates are linked through H_2dien into a three-dimensional network via hydrogen bonds in **1**, while polyoxovanadates are linked by Him into a two-dimensional layer network via hydrogen bonds in **2**. The crystal packing patterns of the two compounds reveal various supramolecular frameworks.

Keywords: Crystal structure; Hydrothermal synthesis; Polyoxovanadates; Protonated diethylenetriamines; Hydrogen bonding; Supramolecular framework

---

1. Introduction

Crystal engineering of organic–inorganic hybrid materials has provoked significant interest because these materials exhibit synergetic properties such as electrical, magnetic and optical properties [1]. A remarkable area is the exploitation of polyoxometalates (POMs) as building blocks to construct the solid-state materials with organic substrates [2–12]. Polyoxovanadates are a prominent subclass of POMs, as compared to polyoxomolybdates and polyoxotungstates, are relatively underinvestigated [13]. In recent years, a number of $[V_{18}O_{42}]$ clusters exhibiting diverse topologies and interesting structural and electronic properties have been reported, including discrete clusters [14], two-dimensional (2-D) networks [4] and three-dimensional (3-D) frameworks [15], etc. The nucleophilic characteristic of the POMs allows specific assembly with electrophilic fragment and it is expected to produce hybrid materials via OH⋯O or NH⋯O hydrogen-bonding interactions. Taking into account of this, a motivation for design and synthesis of organic–inorganic hybrid compounds containing polyoxovanadates and organoamines, has been put forward. Incidentally, hydrogen bonding of conventional OH⋯N and NH⋯O motifs has been the most commonly used an supramolecular cement, yet weaker forces such as CH⋯O, CH⋯N, O⋯I, or even C⋯H and C⋯C have been used [16–18].

In the solid compound, protons in the POM crystals are important in defining the crystal packing through hydrogen bonds [19]. In the POM crystals, protons could prefer the most basic oxygen atoms, which also serve as binding sites

---

*Corresponding author. Fax: +86 431 8499158.
E-mail address: xjq@mail.jlu.edu.cn (J.-Q. Xu).

0022-4596/$ - see front matter © 2007 Elsevier Inc. All rights reserved.
doi:10.1016/j.jssc.2007.04.016

for cationic groups on the POM surface [19]. Both dien and im possess multiple hydrogen bonding sites and several hydrogen bonding assemblies of mononuclear complexes are synthesized [20]. In particular, both dien and im can interact with POMs by hydrogen bonding. Therefore, we chose dien and im as supramolecular modules to assemble polyoxovanadates.

Our investigations have focused on the use of polyoxovanadate as a structural building block in the synthesis of a hydrogen-bonded inorganic–organic high-dimensional structure. Although several organic–inorganic hybrid materials are synthesized (e.g., 2-D $(C_{10}H_{18}N)_4(H_2V_{10}O_{28})\cdot 2DMF\cdot 2H_2O$ [21] and 3-D $[H_2V_{10}O_{28}](H_4bim)_2(H_2O)_4$ [6] ($H_2bim = 2,2'$-bis(4,5-dimethylimidazole)), inorganic–organic hydrogen bonded high-dimensional assembly of octadecavanadate systems has not been reported. In this paper, we report two supramolecular assemblies: $(H_2dien)_4[H_{10}V_{18}O_{42}(PO_4)](PO_4)\cdot 2H_2O$ (**1**) and $(Him)_8[HV_{18}O_{42}(PO_4)]$ (**2**). In this work, based on the same inorganic groups ($V_{18}O_{42}$) in compounds **1** and **2**, their different hydrogen bonding interactions and molecular arrays have been discussed due to their different organoamine. The synthesis of the two organic–inorganic hybrid materials may not only provide hybrid compounds, but also advance the understanding of hybrid materials.

2. Experimental

2.1. General procedures

All chemicals purchased were of reagent grade and used without further purification. C, H, N elemental analyses were performed on Perkin–Elmer 2400 CHN elemental analyzer. Inductively coupled plasma (ICP) analyses were conducted on a Perkin–Elmer Optima 3300 DV spectrometer. Determination of electron spin resonance (ESR) was carried out on Bruker ER 200D-SRC spectrometer. Infrared Spectra were recorded as KBr pellets on a Perkin–Elemer SPECTRUM ONE FTIR spectrophotometer. The TG curve was obtained on a Perkin–Elemer TGA-7000 thermogravimetric analyzer in the flowing air with a temperature ramp rate of 5 °C min^{-1} (for compound 1) and with a temperature ramp rate of 20 °C min^{-1}(for compound 2). An XPS analysis was performed on a VG ESCALAB MKII spectrometer with a Mg*K*α (1253.6 eV) achromatic X-ray source.

2.2. Synthesis

2.2.1. Synthesis of $(H_2dien)_4[H_{10}V_{18}O_{42}(PO_4)](PO_4)\cdot 2H_2O$ (*1*)

Compound **1** was hydrothermally synthesized in 75% yield (based on V). A mixture of $Zn(AC)_2\cdot 2H_2O$(0.36 g, 1.67 mmol), V_2O_5(0.3 g, 1.67 mmol), H_3BO_3 (0.41 g, 3.33 mmol), H_3PO_4 (85 wt%, 0.38 g, 3.33 mmol), dien (1.08 mL, 10 mmol) and H_2O(12 mL, 167 mmol) in a molar ratio of 1:1:2:2:6:100 was neutralized to pH = 6 with KOH under vigorous stirring and sealed in a 15 mL Telfon-lined stainless steal autoclave and heated at 180 °C for 3 days. After cooling to room temperature, black block crystals were isolated, washed with water, and dried at ambient temperature. IR (KBr pellets cm^{-1}) 2924 s, 1591 m, 1444 m, 1183 w, 1053 w, 942 vs, 701 s, 576 w. Calc. for $C_{16}H_{74}N_{12}O_{52}V_{18}P_2$: C, 8.54; H, 3.29; N, 7.47; P, 2.76; V, 40.87%. Found: C, 8.48; H, 3.25; N, 7.40; P, 2.69; V, 40.65%.

2.2.2. Synthesis of $(Him)_8[H\ V_{18}O_{42}(PO_4)]$ (*2*)

Compound **2** was hydrothermally synthesized in 67% yield (based on V). Compound **2** was prepared in the same way as that for **1** but using $NiSO_4\cdot 6H_2O$(0.44 g, 1.67 mmol), $NaH_2PO_4\cdot 2H_2O$(0.26 g, 1.67 mmol), im (0.23 g, 3.3 mmol), $NaBO_2\cdot 4H_2O$(0.46 g, 3.3 mmol) as the reactants. Black block crystals were obtained. IR (KBr pellets cm^{-1}) 3133 vs, 2924 s, 1576 m, 1170 w, 1093 w, 1050 w, 980 m, 936 vs. 704 m, 584 w. Calc. for $C_{24}H_{41}N_{16}O_{46}V_{18}P$: C, 12.91; H, 1.48; N, 10.04; P, 1.39; V, 41.17%. Found: C, 12.97; H, 1.52; N, 10.11; P, 1.42; V, 41.82%.

2.3. X-ray crystallography

The reflection intensity data of **1** were collected on an SMART CCD diffractometer equipped with graphite monochromated MoKα ($\lambda = 0.71073$ Å) radiation at room temperature. A total of 16687 (5976 unique, Rint = 0.0661) reflections of **1** ($-29\leqslant h\leqslant 29$, $-16\leqslant k\leqslant 11$, $-23\leqslant l\leqslant 24$, $1.76<\theta<26.14$) were measured. The reflection intensity data for 2 were collected on a Rigaku R-AXIS RAPID IP diffractometer with graphite monochromated MoKα ($\lambda = 0.71073$ Å) radiation at 293 K. A total of 10,526 (1273 unique, Rint = 0.0236) reflections of **2**($-17\leqslant h\leqslant 18$, $-18\leqslant k\leqslant 17$, $-25\leqslant l\leqslant 14$, $2.13<\theta<29.00$) were measured. Both structures were solved by direct methods and refined using the full-matrix least-squares method on F^2 with SHELXTL-97 crystallographic software package[22,23]. Anisotropic thermal parameters were refined for all non-hydrogen atoms, except O2w in **1**. A summary of the crystallographic data and structure refinements for compounds **1** and **2** are given in Table 1. CCDC reference numbers: 628,467 for **1** and 628,468 for **2**.

3. Results and discussion

3.1. Synthesis

Compound **1** was synthesized from the hydrothermal reaction of $Zn(AC)_2$, V_2O_5, H_3BO_3, H_3PO_4, dien and water in the ratio 1:1:2:2:6:100 at 180 °C for 3 days. When repeating the reaction without boric acid we cannot obtain compound **1**. It has been reported that the $Al(NO_3)_3$ was added during synthesizing the $Na_{10}[H_2W_{12}O_{42}]$ [24]. Taking into account the characteristic comparability of identical group elements we think that the boric acid affects

Table 1
Crystal data and structure refinement parameters for **1** and **2**

Empirical formula	$C_{16}H_{74}N_{12}O_{52}V_{18}P_2$, **1**	$C_{24}H_{41}N_{16}O_{46}V_{18}P$, **2**
Formula weight	2245.73	2237.62
Crystal system	Monoclinic	Tetragonal
Space group	$C2/c$	$I4/mmm$
a (Å)	23.9593(4)	13.5154(8)
b (Å)	13.0098(2)	13.5154(8)
c (Å)	20.1703(4)	19.1136
β (deg)	105.566(3)	90
V (Å^3)	6056.6(19)	3491.4(3)
Z	4	2
Dc (mg m^{-3})	2.463	2.128
Abs. coeff. (mm^{-1})	2.812	2.413
T (K)	293(2)	293(2)
F(000)	4456.0	2188.0
Reflection collected	16,687	10,526
Independent reflections	5976	1273
Goodness-of-fit on F^2	1.031	1.096
Final R indices [$I>2\sigma(I)$]	$R_1 = 0.0423$, $wR_2 = 0.1093$	$R_1 = 0.0607$, $wR_2 = 0.1795$
R indices (all data)	$R_1 = 0.0562$, $wR_2 = 0.1153$	$R_1 = 0.0648$, $wR_2 = 0.1856$
Largest diff. peak and hole (e Å^{-3})	1.260 and −1.136	1.600 and −0.984

$R_1 = \Sigma||F_0|-|F_c||/\Sigma|F_0|$; $wR_2 = [\Sigma|w(F_0^2-F_c^2)/\Sigma|w(F_0^2)^2]^{1/2}$.

the formation of the $[H_{10}V_{18}O_{42}(PO_4)]^{5-}$ cluster although its role is not clear yet. Compound **2** can be obtained under the similar reaction conditions. $NaBO_2$ plays the same role as H_3BO_3 in **1**. The dien and im reactants provide the sources not only of the organoamine cations but also of the reductant for vanadium.

3.2. Structure descriptions

3.2.1. Crystal structure of 1

X-ray crystal structural analysis reveals that compound **1** crystallizes in the monoclinic space group $C2/c$ and is composed of four $[H_2dien]^{2+}$ cations, a $[PO_4]^{3-}$ anion, two water molecules and a octadecavanadate anion $[H_{10}V_{18}O_{42}(PO_4)]^{5-}$ shown in Fig. 1. Fig. 2 shows the hydrogen-bonding network constructed by those four components. Selected bond lengths are listed in Table 2.

The $[H_{10}V_{18}O_{42}(PO_4)]^{5-}$ anion was constructed from a $\{V_{18}O_{42}\}$ [25] shell encapsulating a disordered tetrahedral $\{PO_4\}^{3-}$ group (Fig. 1). The vanadium cluster exhibits only one type of coordination pyramidal V. The host shell was constituted of 18 $\{VO_5\}$ square pyramids by sharing edges through 24μ_3-oxygen atoms. Two kinds of oxygen atoms exist in the host shell, that is, the terminal oxygen O_t and bridging oxygen μ_3–O. The V–O_t bond lengths range from 1.601(3) to 1.643(3) Å, while the V–μ_3–O bond distances range from 1.903(3) to 1.974(4) Å. The central P(2) atom is surrounded by a cube of eight oxygen atoms with each oxygen site half occupied. The P–O_c distances range from 1.500(6) to 1.608(6) Å. More interestingly, there is a $\{PO_4\}^{3-}$ as charge balance anion outside of the shell. The P(1)–O bond lengths vary from 1.505(4) to 1.553(5) Å.

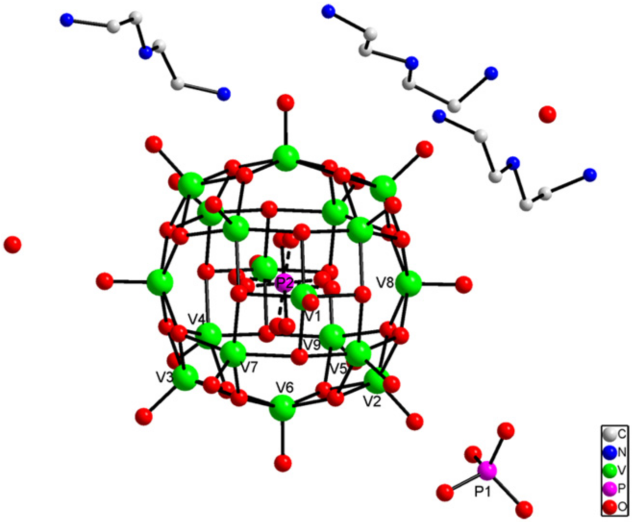

Fig. 1. The building block unit of compound **1** (hydrogen atoms omitted for clarity).

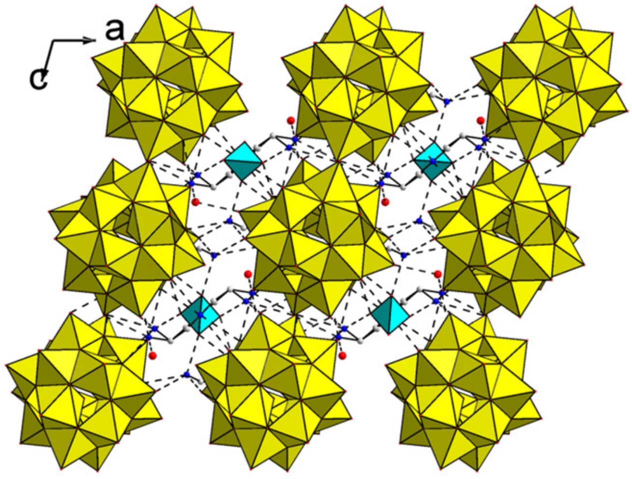

Fig. 2. View of one POM linked by twelve diethylenetriamines in **1**. The polyhedra represent VO_5 (yellow), PO_4 (cyan). The balls represent O (red), C (gray), N (blue) (hydrogen atoms and discrete O1W omitted for clarity).

Bond valence sum calculations [26] show that the 18 V atoms are in the +4 oxidation states [14]. And the two P atoms are in the +5 oxidation states. The bond valence sums (Σs) of 1.28–2.01 for 46 O atoms of the cluster, so the reduction state sum of all O atoms in the cluster is 82. To balance charge, ten additional protons are required, which could not be located experimentally. According to the related vanadium–oxygen clusters of the prototypes $[H_nV_{18}^{IV}O_{42}(X)]^{(13-n)-}$, protonation of the octadecavanadate cluster appears more reasonable and for the purpose of discussion $[H_{10}V_{18}O_{42}(PO_4)]^{5-}$ is assumed [14]. On the basis of the crystallographic studies, we could not establish

Table 2
Selected bond lengths for compound **1**

V(1)–O(9)	1.621(3)	V(8)–O(11)	1.609(3)
V(1)–O(19)	1.904(3)	V(8)–O(14)	1.917(3)
V(1)–O(15)#1	1.906(4)	V(8)–O(17)	1.923(3)
V(1)–O(22)	1.913(3)	V(8)–O(8)	1.937(3)
V(1)–O(21)	1.925(3)	V(8)–O(24)	1.947(3)
V(2)–O(7)	1.620(3)	V(9)–O(16)	1.606(3)
V(2)–O(27)	1.904(3)	V(9)–O(12)	1.942(3)
V(2)–O(8)	1.930(3)	V(9)–O(21)	1.962(3)
V(2)–O(24)	1.933(3)	V(9)–O(24)	1.963(3)
V(2)–O(12)	1.940(4)	V(9)–O(22)	1.965(3)
V(3)–O(18)	1.643(3)	P(1)–O(2)#2	1.505(4)
V(3)–O(17)	1.903(3)	P(1)–O(2)	1.505(4)
V(3)–O(25)	1.906(3)	P(1)–O(1)	1.553(5)
V(3)–O(14)	1.916(3)	P(1)–O(1)#2	1.553(5)
V(3)–O(13)#1	1.974(4)	P(2)–O(5)#1	1.500(6)
V(4)–O(10)	1.614(3)	P(2)–O(5)	1.500(6)
V(4)–O(15)	1.944(3)	P(2)–O(4)#1	1.507(6)
V(4)–O(17)	1.952(3)	P(2)–O(4)	1.507(6)
V(4)–O(21)#1	1.956(3)	P(2)–O(3)	1.529(6)
V(4)–O(13)#1	1.972(3)	P(2)–O(3)#1	1.529(6)
V(5)–O(23)	1.609(3)	P(2)–O(6)#1	1.608(6)
V(5)–O(27)	1.921(3)	P(2)–O(6)	1.608(6)
V(5)–O(8)	1.925(4)	C(1)–N(1)	1.401(9)
V(5)–O(15)	1.938(3)	C(1)–C(2)	1.496(9)
V(5)–O(19)#1	1.959(3)	C(2)–N(2)	1.473(6)
V(6)–O(26)	1.601(3)	C(3)–N(5)	1.465(7)
V(6)–O(27)	1.920(3)	C(3)–C(5)	1.522(7)
V(6)–O(12)	1.929(4)	C(4)–N(3)	1.448(6)
V(6)–O(25)#1	1.939(3)	C(4)–C(6)	1.523(7)
V(6)–O(13)	1.971(3)	C(5)–N(4)	1.491(6)
V(7)–O(20)	1.602(3)	C(6)–N(4)	1.479(6)
V(7)–O(14)	1.931(3)	C(7)–N(6)	1.367(8)
V(7)–O(25)	1.934(3)	C(7)–C(8)	1.453(13)
V(7)–O(19)	1.970(3)	C(8)–N(7)	1.414(12)
V(7)–O(22)	1.973(3)		

Symmetry transformation used to generate equivalent atoms: #1, $-x+1/2$, $-y+1/2$, $-z$. #2, $-x+1$, y, $-z+1/2$.

any of the protonation sites for the anion $[H_{10}V_{18}O_{42}(PO_4)]^{5-}$, which is similar to the reported compound $K_{11}[H_2V^{IV}_{18}O_{42}(Cl)]\cdot 13H_2O\cdot 2N_2H_4$, $K_9[H_4V^{IV}_{18}O_{42}(Br)]\cdot 14H_2O\cdot 4N_2H_4$, $K_9[H_4\ V^{IV}_{18}O_{42}(I)]\cdot 14H_2O\cdot 4N_2H_4$ and $K_{10}[H_3\ V^{IV}_{18}O_{42}(Br)]\cdot 13H_2O\cdot 0.5N_2H_4$ [13].

Fig. 2 shows the interactions of the polyoxovanadate anions with adjacent H_2dien cations. There is extensive hydrogen bonding between the terminal nitrogens of H_2dien and the terminal oxygen atoms from four polyoxovanadate anions as well as three bridging oxygen atoms from polyoxovanadate anions (N1–H1C⋯O22, 2.757 Å; N1–H1D⋯O10, 2.957 Å; N3–H3C⋯O21, 2. 936 Å; N3–H3D⋯O26, 2.929 Å; N3–H3E⋯O19, 3.077 Å; N5–H5C⋯O24, 2.878 Å; N5–H5E⋯O7, 2.847 Å; N7–H7C⋯O12, 2.898 Å; N7–H7D⋯O23, 3.267 Å;), shown in Table 3. Each $[H_{10}V_{18}O_{42}(PO_4)]^{5-}$ anion is linked to sixteen H_2diens and each H_2dien bridges four adjacent $[H_{10}V_{18}O_{42}(PO_4)]^{5-}$ anions via hydrogen bonds. In addition, the medium nitrogen atoms(N2, N4, N6) of H_2dien make hydrogen bonds to the oxygen atoms of $\{PO_4\}^{3-}$ group, and the terminal nitrogen atoms (N1, N5) also make hydrogen bonds to the oxygen atoms of $\{PO_4\}^{3-}$ group (N1–H1E⋯O1, 2.857 Å; N2–H2⋯O1, 2.943 Å; N4–H4⋯O1, 3.026 Å; N5–H5D⋯O2, 2.696 Å; N6–H6⋯O2, 2.958 Å;). There are weak interactions between water molecular and the terminal nitrogen atom(N7) as well as the terminal oxygen atom (O11) of POM (N7–H7E⋯O2w, 2.825 Å; O2w⋯O11, 2.880 Å). Thus, $[H_{10}V_{18}O_{42}(PO_4)]^{5-}$ anion, $\{PO_4\}^{3-}$ group, water molecular and $[H_2\text{dien}]^{2+}$ cation generate a 3-D infinite network via hydrogen bonding interactions (Fig. 2). The hydrogen bonds between H_2dien and POMs are responsible for the formation of the 3-D supramolecular network structure (Table 4).

Table 3
Hydrogen bond lengths (Å) and angles (deg) in **1**

D–H	*d*(D–H)	*d*(H⋯A)	<DHA	*d*(D⋯A)	A
N1–H1C	0.89	1.89	165.4	2.757	O22 [$x+1/2$, $y+1/2$, z]
N1–H1D	0.89	2.16	149.5	2.957	O10 [$x+1/2$, $-y+1/2$, $z+1/2$]
N1–H1E	0.89	2.07	147.4	2.857	O1 [$-x+1$, $y+1$, $-z+1/2$]
N2–H2	0.86	2.19	145.5	2.943	O1 [$-x+1$, $y+1$, $-z+1/2$]
N2–H2	0.86	2.19	145.5	2.943	O1 [x, $y+1$, z]
N3–H3C	0.89	2.07	164.0	2.936	O21[$-x+1/2$,$y+1/2$, $-z+1/2$]
N3–H3D	0.89	2.16	144.6	2.929	O26
N3–H3E	0.89	2.23	158.2	3.077	O19 [x, $y+1$, z]
N4–H4	0.86	2.24	152.1	3.026	O1 [x, $y+1$, z]
N5–H5C	0.89	2.03	158.0	2.878	O24 [$x+1/2$, $y+1/2$, z]
N5–H5D	0.89	1.82	169.6	2.696	O2 [x, $y+1$, z]
N5–H5E	0.89	2.04	150.2	2.847	O7 [$-x+1/2$, $-y+3/2$, $-z$]
N6–H6	0.86	2.21	145.9	2.958	O2 [$x-1/2$, $y+1/2$, z]
N6–H6	0.86	2.21	145.9	2.958	O2 [$-x+1/2$,$y+1/2$, $-z+1/2$]
N7–H7C	0.89	2.03	163.3	2.898	O12
N7–H7D	0.89	2.49	145.7	3.267	O23 [x, $-y+1$, $z+1/2$]
N7–H7E	0.89	2.16	130.8	2.825	O2W [$-x$, $-y+1$, $-z$]

3.2.2. Crystal structure of **2**

The complex $(Him)_8[HV_{18}O_{42}(PO_4)]$ (**2**) consists of an $[HV_{18}O_{42}(PO_4)]^{8-}$ POM and eight $[Him]^+$ cations and crystallizes in the tetragonal space group *I*4/*mmm*. $[HV_{18}O_{42}(PO_4)]^{8-}$ of compound **2** has the identical V_{18} structure as $[H_{10}V_{18}O_{42}(PO_4)]^{5-}$ of **1** (Fig. 3). In the POM of **2**, the P–O_c bond distance is 1.5382(19) Å. The V–O distances can be grouped into two sets V–O_t (terminal) 1.6109(11)–1.625(2) Å, and V–O_b (bridge) 1.9034(13)–1.9393(9) Å.

Table 4
Selected bond lengths for compound **2**

V(1)–O(1)	1.625(2)	V(4)–O(4)#8	1.9337(6)
V(1)–O(3)#1	1.9055(8)	V(4)–O(3)	1.9393(9)
V(1)–O(3)	1.9055(8)	V(4)–O(3)#1	1.9393(9)
V(1)–O(3)#2	1.9055(8)	P(1)–O(7)#10	1.5382(19)
V(1)–O(3)#3	1.9055(8)	P(1)–O(7)#8	1.5382(19)
V(2)–O(2)	1.6124(16)	P(1)–O(7)#11	1.5382(19)
V(2)–O(3)	1.9291(8)	P(1)–O(7)#9	1.5382(19)
V(2)–O(3)#5	1.9291(8)	P(1)–O(7)#3	1.5382(19)
V(2)–O(3)#6	1.9291(8)	P(1)–O(7)#7	1.5382(19)
V(2)–O(3)#3	1.9291(8)	P(1)–O(7)#4	1.5382(19)
V(3)–O(5)	1.620(3)	P(1)–O(7)	1.5382(19)
V(3)–O(4)#8	1.9034(13)	O(4)–V(4)#7	1.9337(6)
V(3)–O(4)	1.9034(13)	C(1)–N(1)	1.324(3)
V(3)–O(4)#7	1.9034(13)	C(1)–N(1)#12	1.324(3)
V(3)–O(4)#9	1.9034(13)	C(2)–N(1)	1.111(4)
V(4)–O(6)	1.6109(11)	C(2)–C(2)#12	1.382(6)
V(4)–O(4)	1.9337(6)		

Symmetry transformation used to generate equivalent atoms: #1, −*y*, *x*, *z*. #2, *y*, −*x*, −*z*. #3, −*x*, −*y*, *z*. #4, *x*, *y*, −*z*. #5, *y*, −*x*, *z*. #6, −*x*, *y*, −*z*. #7, −*x*, *y*, *z*. #8, *y*, *x*, −*z*. *y*, *x*, *z*. #10, −*x*, −*y*, −*z*. #11, −*y*, *x*, −*z*. #12, −*x*+1, *y*, *z*.

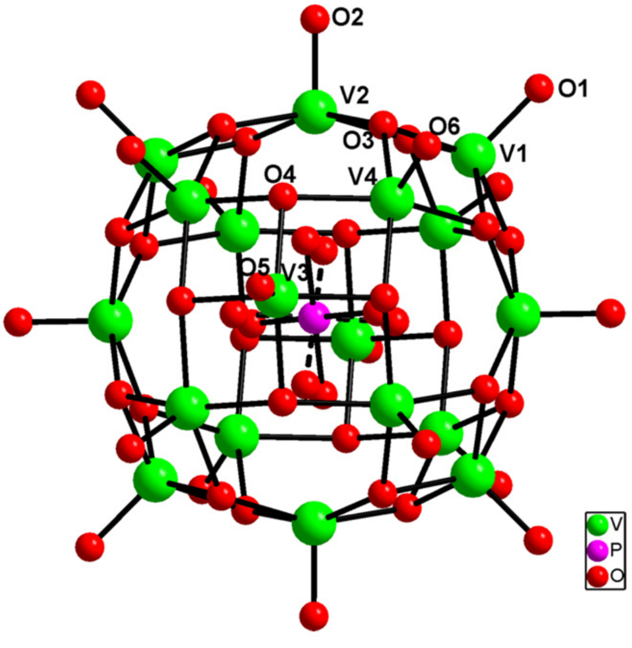

Fig. 3. A view of the anion cluster $[HV_{18}O_{42}(PO_4)]^{8-}$ in the crystal of **2** showing the atom labeling scheme.

Bond valence sum calculations [26] on the V coordination spheres give a valence of 4.461 for V (1), 4.330 for V (2), 4.503 for V (3) and 4.278 for V (4), respectively. The average oxidation state is 4.355 (expected value for $V^{V}_{6}V^{IV}_{12}$ is 4.333), suggesting that the $3d^1$ electrons in **2** are delocalized. To balance charge, one additional proton is required, which could not be located experimentally.

There is only one kind of hydrogen bonding between the nitrogen atoms of Hims and the terminal oxygen atoms of POMS (N1–H1A···O6 3.227 Å). Each O6 of POM linked to two protonated ims. While the $[HV_{18}O_{42}(PO_4)]^{8-}$ anion has eight O6 atoms. Hence one $[HV_{18}O_{42}(PO_4)]^{8-}$ anion forms hydrogen bonds with 16 Him cations and each Him links two adjacent $[HV_{18}O_{42}(PO_4)]^{8-}$ anions, resulting in a layered structure (Fig. 4(a)). This layer is arranged parallel to the crystallographic *ab* plane (see in Fig. 4(a)). In the layer, through the hydrogen bonding of four Him cations,

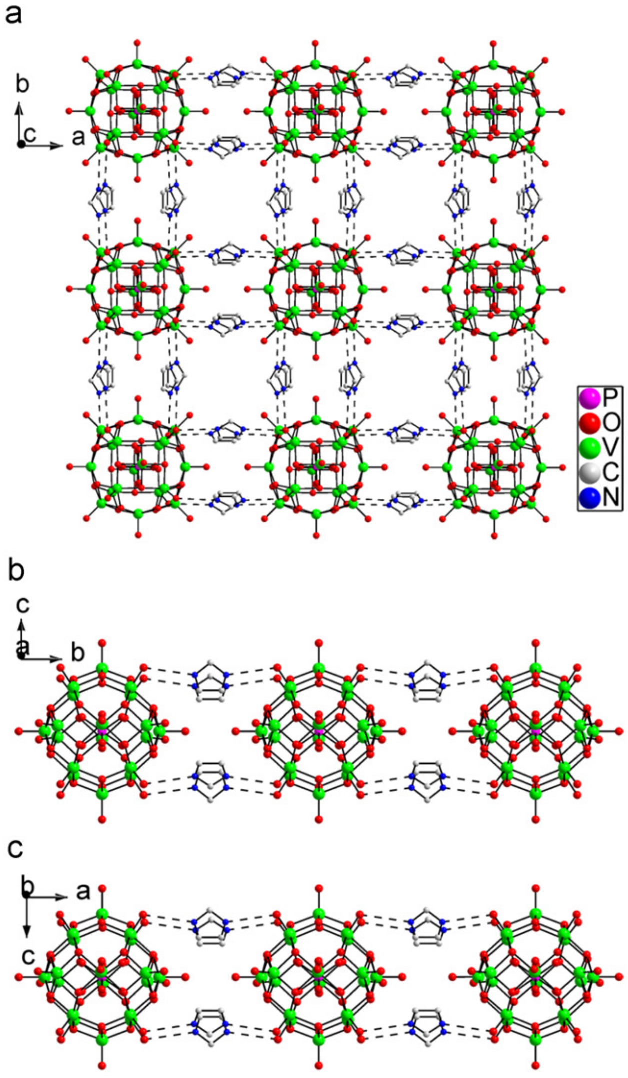

Fig. 4. (a) A view of the supramolecular layer of compound **2** down the *c*-axis showing the four ims between two adjacent clusters, (b) the straight chain of compound **2** extending along the *a*-axis, and (c) the straight chain of compound **2** extending along the *b*-axis.

the clusters are linked to one another along the *a*- or *b*-axis into a novel straight chain, as shown as in Fig. 4(b) and (c), the two different directional one-dimensional (1-D) straight chain are arranged in a cross-like fashion, resulting in the 2-D supramolecular array (Fig. 4(a)).

3.3. Characterization of the compounds

The ESR spectra for compounds **1** and **2** were recorded at room temperature (298 K) on crystalline samples shows the V^{IV} signals with $g = 1.97$ for compound **1**(S, Fig. 1), and $g = 1.96$ for compound **2**(S, Fig. 2), being consistent with the results of valence sum calculations of compounds **1** and **2**.

Fig. 5(a) shows the XPS [27] spectrum of **1** in the V 2*p* region, with one peak at 515.86 eV being ascribed to V^{4+}. XPS for compound **2** (Fig. 5(b)) gives two peaks at 516.06 and 517.74 eV attributted to V^{4+} $2p_{3/2}$ and V^{5+} $2p_{3/2}$, respectively. By comparing Fig. 5(a) with Fig. 5(b), we can see the half peak width of Fig. 5(a) is narrower than the peak width of Fig. 5(b). It shows the vanadium atoms of compound **1** have single oxidation states, and the vanadium atoms of compound **2** have mixed oxidation states. The XPS estimation of the valence-state values seems to be in reasonable agreement with those calculated from the bond valence sum calculations. These results further confirm the valences of the vanadium atoms.

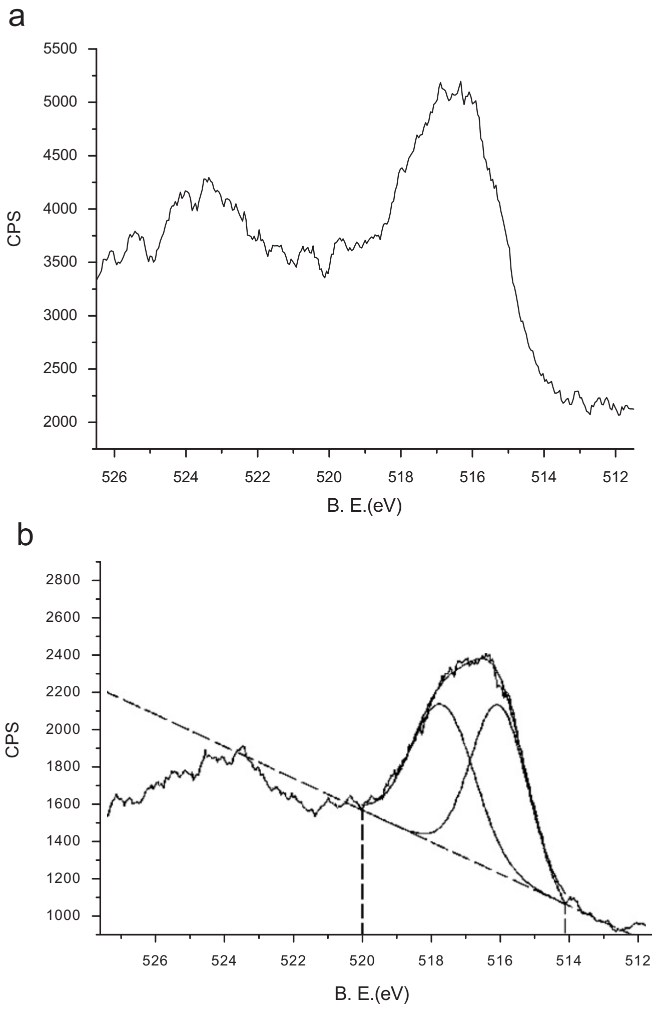

Fig. 5. (a) XPS for V^{IV} in compound **1** and (b) XPS for V^{IV}–V^{V} in compound **2**.

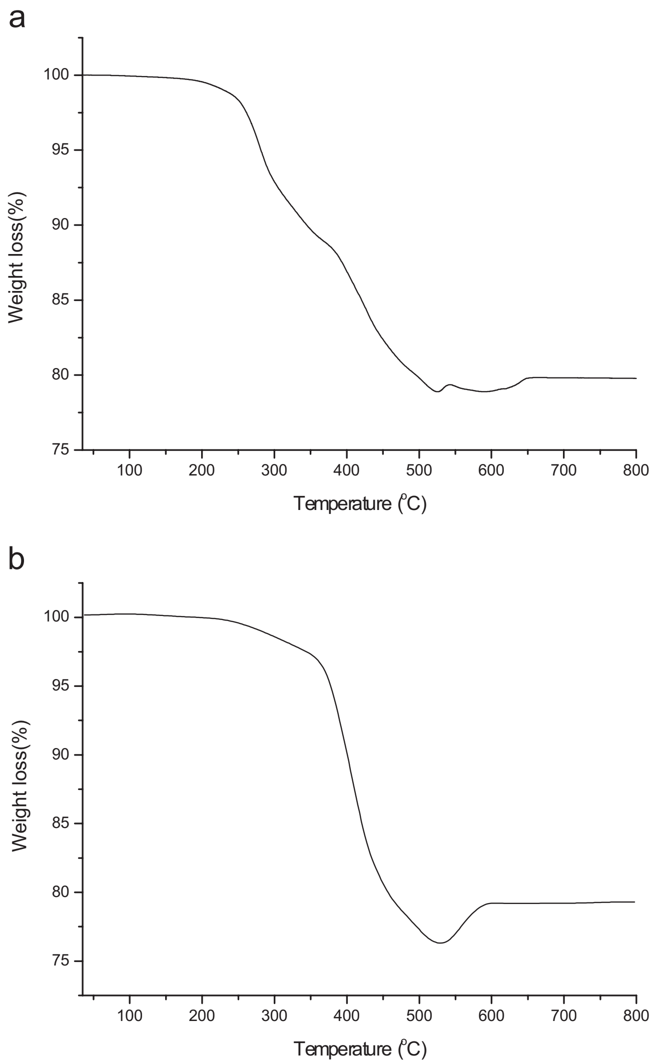

Fig. 6. (a) TG curve of $(H_2dien)_4[H_{10}V_{18}O_{42}(PO_4)](PO_4)\cdot 2H_2O$ (**1**) and (b) TG curve of $(Him)_8[H\,V_{18}O_{42}(PO_4)]$ (**2**).

The TG analyses of the two compounds are performed in the temperature range of 35–800 °C. In the range of 118–527 °C, compound **1** loses its crystal water and H_2dien. The weight loss of this step is 21.25% which is in good accordance with the calculated value (20.75%). Upon further heating, a continuous weight increase corresponds to uptake of oxygen accompanied by valence state change of vanadium ions (see in Fig. 6(a)). There was no further weight change up to 800 °C. From 200 to 530 °C, the weight loss of **2** is 24.43% (calculated value: 24.44%), corresponding to the release of Him. Between 535 to 572 °C, the slight increase of weight clearly indicates the occurrence of an oxidative process. Upon further heating, there was no weight change for **2** (see in Fig. 6(b)).

4. Conclusion

In summary, we have described two unique compounds exhibiting that the polyoxovanadates and organoamines are linked together via various hydrogen bonds. The hydrogen bonding interactions between POMs and H_2dien and Him in the two structures, respectively have been discussed in details. Evidently, hydrogen bonds in the complexes enhance the stability of the structure [21]. In comparison with **1** and **2**, we can make a conclusion the basic building block unit in **1** and **2** have the similar structure.

Acknowledgments

This work was supported by National Natural Science Foundation of China (20333070 and 20571032).

Appendix A. Supplementary materials

Supplementary data associated with this article can be found in the online version at doi:10.1016/j.jssc.2007.04.016.

References

[1] C.R. Kagan, D.B. Mitzi, C.D. Dimitrakopoulos, Science 286 (1999) 945–947.

[2] D. Attanasio, M. Bonamico, V. Fares, P. Imperatori, L.J. Suber, J. Chem. Soc. Dalton Trans. (1990) 3221–3228.

[3] C.M. Liu, D.Q. Zhang, M. Xiong, D.B. Zhu, Chem. Commun. (2002) 1416–1417.

[4] C.L. Pan, J.Q. Xu, G.H. Li, X.B. Cui, Y. Le, G.D. Yang, Dalton Trans. (2003) 517–518.

[5] M.I. Khan, E. Yohannes, R.J. Doedens, Inorg. Chem. 42 (2003) 3125–3129.

[6] H. Kumagai, M. Arishima, S. Kitagawa, K. Ymada, S. Kawata, S. Kaizaki, Inorg. Chem. 41 (2002) 1989–1992.

[7] M.I. Khan, S. Ayesh, R.J. Doedens, M. Yu, C.J. O'Connor, Chem. Commun. (2005) 4658–4660.

[8] J.Q. Xu, R.Z. Wang, G.Y. Yang, Y.H. Xing, D.M. Li, W.M. Bu, L. Ye, Y.G. Fan, G.D. Yang, Y. Xing, Y.H. Lin, H.Q. Jia, Chem. Commun. (1999) 983–984.

[9] S.T. Zheng, J. Zhang, G.Y. Yang, Inorg. Chem. 44 (2005) 2426–2430.

[10] X.B. Cui, J.Q. Xu, H. Meng, S.T. Zheng, G.Y. Yang, Inorg. Chem. 45 (2004) 8005–8009.

[11] Y. Lu, Y. Xu, E.B. Wang, J. Lü, C.W. Hu, L. Xu, Cryst. Growth Des. 5 (2005) 257–260.

[12] D. Rehder, Mol. Eng. 3 (1993) 1–3.

[13] W.G. Klemperer, T.A. Marquart, O.M. Yaghi, Angew. Chem. Int. Ed. Engl. 31 (1992) 49–51.

[14] A. Müller, R. Sessoli, E. Krickemeyer, H. Bögger, J. Meyer, D. Gatteschi, L. Pardi, J. Westphal, K. Hovemeier, R. Rohlfing, J. Döring, F. Hellweg, C. Beugholt, M. Schmidtmann, Inorg. Chem. 36 (1997) 5239–5250.

[15] M.I. Khan, E. Yohannes, R.J. Doedens, Angew. Chem. Int. Ed. Engl. 38 (1999) 1292–1294.

[16] J.C. MacDonald, G.M. Whitesides, Chem. Rev. 94 (1994) 2383–2420.

[17] G.R. Desiraju, Angew. Chem. Int. Ed. Engl. 34 (1995) 2311–2327.

[18] M. Tadokoro, K. Isobe, H. Uekusa, Y. Ohashi, J. Koyoda, K. Tashiro, K. Nakasuji, Angew. Chem. Int. Ed. 38 (1999) 95–98.

[19] T. Ozeki, T. Yamase, H. Naruke, Y. Sasaki, Bull. Chem. Soc. Jpn. 67 (1994) 3249–3255.

[20] R.L. Fanshawe, A. Mobinikhaledi, C.R. Clark, A.G. Blackman, Inorg. Chim. Acta 307 (2000) 26–31.

[21] J. Yang, K.L. Huang, Z.F. Pu, Y. Gong, H. Li, C.W. Hu, J. Mol. Struct. 789 (2006) 162–168.

[22] G.M. Sheldrick, SHELXS 97, Program for Crystal Structure Solution, University of Göttingen, Göttingen, Germany, 1997.

[23] G.M. Sheldrick, SHELXS 97, Program for Crystal Structure Refinement, University of Göttingen, Göttingen, Germany, 1997.

[24] H.T. Evans Jr., O.W. Rollins, Acta Crystallogr. Sect. B 32 (1976) 1565–1567.

[25] A. Müller, M. Penk, R. Rohlfing, E. Krickemeyer, J. Döring, Angew. Chem. Int. Ed. Engl. 29 (1990) 926–927.

[26] I.D. Brown, in: M. O'Keeffe, A. Navrotsky (Eds.), Structure and Bonding in Crystals, vol. 2, Academic Press, New York, 1981.

[27] C.D. Wagner, W.M. Riggs, L.E. Davis, J.F. Moulder, G.E. Muilenberg, Handbook of X-ray Photoelectron Spectroscopy, Perkin–Elmer Corp., Michigan, 1978.